

**Superconducting Transition and Heterodyne Performance at 730 GHz
of a Diffusion-cooled Nb Hot-electron Bolometer Mixer**

J.R. Gao^{a,b}, M.E. Glastra^a, R.H. Heeres^a, W. Hulshoff^b, D. Wilms Floet^a,
H. van de Stadt^b, T.M. Klapwijk^a and Th. de Graauw^b

^a Department of Applied Physics and Materials Science Center, University of Groningen,
Nijenborgh 4, 9747 AG Groningen, The Netherlands

^b Space Research Organization of the Netherlands, PO Box 800, 9700 AV Groningen
The Netherlands

Abstract

We report two typical experimental results of waveguide diffusion-cooled Nb hot-electron bolometer (HEB) mixers. The device is a thin (10 nm) Nb bridge with a length of 0.3 μm and a width of 0.9 μm and is defined using photolithography. In the first experiment, the resistance of a HEB is studied as a function of temperature. We observe two critical temperatures, which correspond to the T_c of the Nb bridge and the T_c of the Nb under the Au pads, respectively. These two T_c define a superconducting transition width ΔT of a HEB. The reduced T_c of the Nb under the Au pads is explained by the superconducting proximity effect. In the second experiment, we measure relative conversion efficiency vs intermediate frequency (IF) by using two coherent sources, a carcinotron and a Gunn oscillator, and determine an IF roll-off ($IF_{roll-off}$) between 0.6 and 1.2 GHz, in agreement with a value estimated in terms of the diffusion-cooled model.

1. Introduction

Recent work on diffusion-cooled Nb hot-electron bolometer (HEB) mixers reported by the Jet Propulsion Laboratory and other groups¹⁻⁵ has demonstrated that they are promising heterodyne detectors in the THz frequency range. It has been shown that HEB mixers have low noise and a reasonable wide intermediate frequency roll-off ($IF_{roll-off}$), but no clear upper limit of operating frequency and no requirement of high local oscillator (LO) power. HEB mixers are expected to compete with NbN SIS mixers around 1.5 THz, but to be superior at much higher frequencies. It is known that coupling a signal at radio frequency (RF) and a signal from a LO to a superconducting HEB can generate a response at IF frequency, provided that the superconductor is biased near the middle point of the transition due to the heating of LO and DC power. So a superconducting HEB can be operated as a mixer. For a practical HEB mixer, it is required that an $IF_{roll-off}$, defined as the IF frequency at which the relative conversion efficiency decreases by 3 dB, should be ≥ 1.5 GHz. A diffusion-cooled Nb HEB suggested by Prober¹ can satisfy this requirement because the hot electron are cooled via out-diffusion, but not via electron-phonon process. This new cooling process can result in a shorter thermal response time and thus a higher $IF_{roll-off}$. A typical diffusion-cooled HEB consists of a thin (~ 10 nm) and narrow (~ 100 nm) superconducting Nb bridge, which is attached to two Au pads serving as heat sinks. The separation of the two pads defines the bridge. A short bridge (~ 200 nm) is needed to ensure a fast out-diffusion

cooling.

Several heterodyne measurements have been reported using diffusion cooled Nb HEBs. Those are in the waveguide mixers at 530 GHz² and in quasi-optical mixers at 1.3 THz³ using double dipole antenna by Skalare *et al.*, in quasi-optical mixers at 2.5 THz using twin-slot antenna by Karasik *et al.*⁴, and waveguide mixers at 800 GHz by Fiegle *et al.*⁵. Also, the dependence of $IF_{roll-off}$ on bridge length is studied by Burke *et al.*⁶ and the output noise spectrum by Schoelkopf *et al.*⁷.

It is known theoretically that the superconducting transition width ΔT of a HEB and details of resistance vs temperature within the ΔT play a critical role in determination of mixer properties, such as conversion efficiency, mixer noise temperature and requirement of LO power. However, the origin of the transition is not clear. In this paper we will address this basic problem and also report measurements of the $IF_{roll-off}$. Furthermore, we will present our preliminary receiver noise measurements around 730 GHz.

2. Devices and Fabrication

Part of the HEB device is schematically illustrated in Fig. 1a. It consists of a Nb strip with a thickness of 10 nm and a width of 0.9 μm , attached to two Au contact pads (60 nm thick), acting as heat-sinks and RF probes. The separation of the Au contact pads in this case is 0.3 μm , defining the bridge length. The devices are fully fabricated using the standard photolithography and realized in the following way. Starting with a fused quartz wafer, a 10 nm thick Nb is sputtered over the whole area. The Au pads are patterned using photolithography, followed by an Au sputtering deposition and a lift-off process. To remove the native oxides of Nb, a short RF Ar sputter etching of 1 min is applied before the Au deposition. To improve adhesion we add a thin (6 nm) Al layer between Nb and Au. Then the choke structure, which is a Nb and Au bilayer, is defined by sputtering and a lift-off process. The Au layer is for electrical contacts and to prevent Nb etching during the last step. In this last step, bridges are formed by etching the Nb and applying photoresist as a mask. Fig. 1b gives a SEM micrograph of a completed HEB. Before heterodyne measurements, devices are diced and polished so that the substrate has a width of 90 μm and a thickness of 50 μm .

There are two points we need to explain here. Firstly, to establish film growing parameters for Nb thin films we choose a simple fabrication process, namely the photolithography. The present process can lead to bridge dimensions as small as 300 nm. Secondly, since $IF_{roll-off}$ is determined by both the bridge length and interfaces between Au and Nb, it is essential to form an oxide-free interface. For the devices studied, we apply a RF Ar sputter etching of 1 min, which is shorter than the standard process for Nb SIS (2.5 min). Thus, we expect a possible reduction of $IF_{roll-off}$, although we do not have clear evidence of oxide barriers from the DC measurements.

3. DC Measurements and Superconducting Transition

The resistance (R) of a HEB is measured as a function of temperature (T) by applying a standard lock-in technique using a low current. The sample is mounted in a dipstick with a vacuum can and the temperature is varied by changing heating currents. Fig. 2 shows R vs T curves for two different devices. Below 5.5 K the resistance is zero and above 6.5 K it reaches the normal state resistance R_N . Between these two temperatures the resistance increases with temperature. We will explain that in our case the two values, 5.5 K and 6.5

K, correspond to the critical temperature $T_c(\text{Nb/Au})$ of Nb under the Au contacts and the critical temperature $T_c(\text{Nb})$ of the Nb bridge, respectively. The difference between the $T_c(\text{Nb})$ and the $T_c(\text{Nb/Au})$ defines the transition width ΔT of a HEB. The low $T_c(\text{Nb/Au})$ is due to the superconducting proximity effect. This conclusion is supported by additional measurements and a numerical calculation.

The different R_N values between the two devices in fig. 2 are due to the difference in bridge size, which is negligible if devices are close to each other on the wafer.

The first experimental result to support our conclusion is the measurement of R vs T for Nb films with different thicknesses or different levels of impurities. The latter is manipulated by using different sputtering rates. We find that the Nb films have a transition width ΔT smaller than 0.1 K regardless of thickness and sputtering rate. In general, a lower sputtering rate can cause a reduction of T_c . The reason for this is that more contaminations existing in the background of a sputtering system are introduced to the film. Very likely, the presence of oxygen and water in the sputtering system is the cause of the reduction⁹. Reducing the thickness gives the same effect.

The second experimental result¹⁰ to support our conclusion is the separate measurement performed in a device structure allowing determination of the $T_c(\text{Nb})$ and the $T_c(\text{Nb/Au})$ simultaneously. We observe a reduced $T_c(\text{Nb/Au})$.

We calculate the reduction of T_c using a model by Werthamer⁸ based on the proximity effect. Fig. 3 shows the calculated normalized critical temperature T_c/T_{c0} of Nb under Au or Al layer as a function of metal thickness D_n . Details of the numerical calculation are given elsewhere¹⁰. For comparison, our experimental data, together with the data from others¹¹, are included. As expected, the T_c of Nb will decrease with increasing the metal thickness. It is also clear that this reduction depends on which metal is used. The difference between Au and Al is mainly caused by the fact that Al is a superconductor and Au not. We notice from our calculations that the parameters, the electronic specific heat γ for Nb and T_{c0} for Al, have a clear influence on T_c . However, we find that varying the electron mean free path for Al or Au gives only little effects.

The quantitative difference between the calculated and experimental results is obvious. One possible reason is that, as mentioned before, the native oxide layer may not be fully removed. This would cause a less transparent interface and weaken the proximity effect. There is also another complication. For our devices, there is a very thin Al layer between Nb and Au. The influence for this layer is not clear. But it is reasonable to assume that the result should be close to one calculated for an Au layer.

So far we only explain the double T_c characteristic. Another interesting feature, that is the temperature dependence of the resistance within the transition width ΔT , is probably also a result of the proximity effect. However, in this case, we have to deal with the proximity effect along the bridge, by considering the Nb bridge as a *superconductor* and the contacts which are Nb/Au bilayer as a *normal metal*. Unfortunately, such a system is beyond Werthamer's theory. A different model is required to extend our calculations.

4. Heterodyne Measurements

4.1 Heterodyne Measurement Setup

The heterodyne measurements are performed in a modified waveguide receiver test setup originally designed for Nb SIS mixers. The waveguide mixer block has been previously used for Nb SIS mixers around 700 GHz^{12,13}. Major modifications are made with respect to the bias-T connector and the IF chain. For the former a bias-T connector suitable for 0.1 to 4

GHz is chosen and for the latter Miteq wide-band low temperature FET amplifiers are used. For the Y-factor measurements, an amplifier¹⁴ operating between 0.1 to 2 GHz with a noise temperature of 15 K at liquid nitrogen temperature, together with two room-temperature amplifiers operating between 0.1- 1 GHz, is used. A low pass filter of 0.5 GHz is applied to limit the bandwidth for the receiver noise measurements to 0.1-0.5 GHz. For the $IF_{roll-off}$ measurements, the second amplifier (0.1 to 8 GHz) with a gain flatness of ± 1.5 dB (max.) is used in combination with a room temperature amplifier with the same bandwidth.

Three different local oscillators are employed, a carcinotron, a backward wave oscillator (BWO), and a Gunn oscillator.

4.2 FTS Response

As the first step to characterize HEB mixers, we evaluate the direct response of a HEB using a Fourier transform spectrometer (FTS). The normal state resistance of the device is 13Ω . The measurements are done by raising the temperature of a HEB within the transition region. Although they can also be performed at the bath temperature, signals are less stable. Fig. 4 shows FTS direct response spectra, different curves corresponding to different positions of the backshort tuner. The continuous curve corresponds to the case that the backshort is close to the HEB. Peak response, as expected, takes place at around 700 GHz. It is evident that the HEB mixer has a much wider instantaneous bandwidth than SIS mixers. The response starts around 500 GHz, which is the waveguide cut-off frequency, and ends around 960 GHz, where the RF loss through the substrate channel may become significant. It is worthwhile to note that, in contrast to SIS mixers, the instantaneous bandwidth is not set by the HEB mixer, but set by the waveguide, or by an antenna in the case of quasi-optical HEB mixers^{3,4}. In the FTS spectra a dip at 750 GHz is due to water vapour absorption.

4.3 Determination of $IF_{roll-off}$

We study relative conversion efficiency vs IF by mixing the two monochromatic signals from a carcinotron and a Gunn oscillator. The former is used as a LO to pump the mixer, while the latter acts as a RF signal. Their frequencies are chosen around 700 GHz and their frequency difference specifies an intermediate frequency. Mixed signals are monitored with a spectrum analyser. The measurements are carried out at $T_{bath}=4.6$ K, which is read from a temperature sensor placed in the mixer block.

The amplitude of the mixed signal as a function of IF is measured by varying the LO frequency, but keeping the pumping power constant. The power is monitored through ΔI (at a constant bias voltage) which is the current difference with and without the LO power. The pumping power is chosen in such a way that the output of the mixed signal is maximal. Fig.5 illustrates the normalized amplitude of the mixed signal as a function of IF for two different bias voltages, 0.25 and 0.35 mV. No corrections are applied for small fluctuations in the gain of the IF chain. We fit the theoretical expression for the frequency dependence of the conversion efficiency, $[1+(f_{IF}/IF_{roll-off})^2]^{-1}$, to the experimental data. We find that our data obey the function reasonably well and obtained an $IF_{roll-off}$ of 0.6 GHz at 0.25 mV and 0.9 GHz at 0.35 mV. For the same device we also determined the $IF_{roll-off}$ at a lower temperature (3 K) and higher bias voltages. Depending on the bias voltage, the $IF_{roll-off}$ ranges from 0.6 to 1.2 GHz. No clear differences are found between 3 and 4.6 K.

In another measurement we used a combination of a carcinotron and a BWO. Due to the BWO the mixed signal is broad (80 MHz). By taking the averaged signal amplitude the results still show similar behaviour as previous ones.

It is known that the $IF_{roll-off}$ for a HEB follows $IF_{roll-off} = (2\pi \tau_{th})^{-1}$, where is the thermal response time $\tau_{th} = C/G$. Here C is the thermal capacitance of a HEB and G the thermal

conductance. To calculate the $IF_{roll-off}$, we need to know the C and G . We calculate the C value using $C=\gamma TV$, where γ is the coefficient of electronic specific heat ($700 \text{ J/K}^2\text{m}^3$); T critical temperature of the bridge (6.5 K); and V volume ($2.7 \times 10^{-21} \text{ m}^3$). We estimate the G value of a HEB, fabricated in the same wafer but with $R_N=23 \Omega$, by measuring the resistance as a function of temperature for different currents^{10,13}. In this case G equals 32 nW/K . Since the resistance of the device used for the $IF_{roll-off}$ measurement is 13Ω , we find the G value being 57 nW/K by scaling the resistances. In this way, we derive a τ_{th} of 0.21 ns and thus an $IF_{roll-off}$ of 0.8 GHz . This value is roughly in agreement with those of the $IF_{roll-off}$ measurements. Since the experimental $IF_{roll-off}$ values are much higher than that one would expect from electron-phonon cooling HEBs⁶, we conclude that the cooling process in our devices is indeed dominated by diffusion.

We notice that, if we calculate the G by using the Wiedemann-Franz law, the $IF_{roll-off}$ should be 2.5 GHz for the present device. There are several possible reasons to explain the difference. Firstly, the interfaces may, as mentioned before, not be highly transparent. We expect that, if we take a long RF sputter etching time before the deposition of the Au pads, this effect can be diminished. Secondly, since the operating temperature is below the $T_c(\text{Nb/Au})$ (the Nb under the Au pads), this Nb is likely still superconducting, although the Nb bridge can be in the resistive state due to LO pumping. Because of the presence of superconductor/metal interfaces, hot electrons may have difficulties to diffuse out. Finally, variations in bridge length (see fig. 1b) due to mis-alignment of photolithography can certainly have an additional effect.

4.4 Receiver Noise Measurements

Fig. 6 shows a Y -factor measurement of the HEB mixer together with the pumped I-V curve at a LO frequency of 730 GHz and $T_{bath}=4.6 \text{ K}$. Here ac output power is a measure of the response between hot and cold loads and is proportional to the Y -factor. The LO power that pumps the HEB, is supplied by a carcinotron. The maximum Y -factor is 0.18 , giving a receiver noise temperature of 5500 K . Since this is a very preliminary measurement, we will not discuss this result further before we have optimized the IF chain. One interesting feature that needs to be discussed is the operating bias point. We can see clear hot/cold response only at bias voltages below the drop-back point, which differs from the results reported by others²⁻⁵. In other words, if we use the current-bias mode for measurements, it is difficult to measure response in the IF output. For this reason, all the measurements are performed in the voltage-bias mode.

4.5 Local Oscillator Power

We estimate LO power using a technique commonly applied for HEBs¹⁵. The coupled LO power is approximately given by the difference in DC heating power taken from two points (from a constant resistance line) in the pumped and unpumped curves, respectively. We find that the coupled LO power is 130 nW at 4.6 K and 160 nW at 3 K for the $IF_{roll-off}$ measurements, and is about 90 nW for the receiver noise temperature measurement.

5. Conclusions

We fabricate waveguide diffusion-cooled Nb HEB mixers using photolithography. Two basic aspects have been studied. Firstly, the resistance of a HEB is studied as a function of temperature. We observe two critical temperatures, which correspond to the T_c of the Nb

bridge and the T_c of the Nb under the Au pads, respectively. For a HEB these two T_c define a superconducting transition width. In our case the ΔT equals about 1 K. The origin of the transition is interpreted by the superconducting proximity effect. Secondly, we measure relative conversion efficiency vs intermediate frequency by mixing two coherent signals and obtain an $IF_{roll-off}$ ranging from 0.6 to 1.2 GHz, which is in agreement with the value estimated in terms of the diffusion-cooled model. Furthermore, the first noise measurements show a receiver noise temperature (DSB) of 5500 K at 730 GHz. For all the measurements the local oscillator power needed is ≤ 160 nW.

ACKNOWLEDGEMENT: The authors would like to thank S. Bakker for performing photolithography, J.B.M. Jegers for his assistance in sputtering and RIE etching, and H. Schaeffer and H. Golstein for their assistance in measurements. We also would like thank P.R. Wesselius and P.A. J. de Korte for their support and encouragement. This work is financially supported by the Stichting voor Technische Wetenschappen (STW).

References

1. D.E. Prober, *Appl. Phys. Lett.* **62**, 17 (1993).
2. A. Skalare, W.R. McGrath, B. Bumble, H.G. LeDuc, P.J. Burke, A.A. Verheijen and D.E. Prober, *Appl. Phys. Lett.* **68**, 1558(1996).
3. A. Skalare, W.R. McGrath, B. Bumble, and H.G. LeDuc, *IEEE Trans. Appl. Super.* 1997 (in press).
4. B.S. Karasik, M.C. Gaidis, W.R. McGrath, B. Bumble, and H. G. LeDuc, *IEEE Trans. Appl. Super.* 1997 (in press).
5. K. Fiegle, D. Diehl, and K. Jacobs, *IEEE Trans. Appl. Super.* 1997 (in press).
6. P.J. Burke, R.J. Schoelkopf, D.E. Prober, A. Skalare, W.R. McGrath, B. Bumble, and H.G. LeDuc, *Appl. Phys. Lett.*, **68**, 3344(1996)..
7. R.J. Schoelkopf, P.J. Burke, D.E. Prober, A. Skalare, B. Karasik, W.R. McGrath, M.C. Gaidis, B. Bumble, and H.G. LeDuc, *IEEE Trans. Appl. Super.* 1997 (in press).
8. N.R. Werthamer, *Phys. Rev.* **132**, 2440 (1963); J.J. Hauser, H.C. Theuerer and N.R. Werthamer, *Phys. Rev.* **136**, A637 (1964).
9. C.C. Koch, J.O. Scarbrough, and D.M. Kroeger, *Phys. Rev.* **B9**, 888(1974).
10. R.H. Heeres, *M. Sc. thesis*, University of Groningen, The Netherlands, 1996.
11. A. Skalare, W.R. McGrath, B. Bumble, H.G. LeDuc, P.J. Burke, A.A. Verheijen and D.E. Prober, *Proc. 5th Int. Symp. on Space Terahertz Technology*, p. 157, May 10-12, 1994, Univ. of Michigan, Ann Arbor, Michigan; and P. J. Burke, private communication.
12. G. de Lange, C.E. Honingh, J.J. Kuipers, H.H. A. Schaeffer, R.A. Panhuyzen, T.M. Klapwijk, H. van de Stadt and Th. de Graauw, *Appl. Phys. Lett.* **64**, 3039 (1994).
13. H. van de Stadt, A. Baryshev, P. Dieleman, J.R. Gao, H. Golstein, Th. de Graauw, W. Hulshoff, T.M. Klapwijk, S. Kovtonyuk, and H. Schaeffer, *Proc. 30th ESLAB Symp. On Submillimetre and Far-Infrared Space Instrumentation*, 231, 1996, Noordwijk, The Netherlands.
14. On the amplifier, we applied a bias voltage of 5 V, as suggested by Miteq. However, we later noticed that a bias of 3-4 V may improve S/N ratio and also reduce the power. The gain is reduced slightly.
15. H. Ekström, B. Karasik, E. Kollberg, and K.S. Yngvesson, *Proc. 5th Int. Symp. on Space Terahertz Technology*. p.169, May, 1994, Univ. of Michigan, Ann Arbor, Michigan

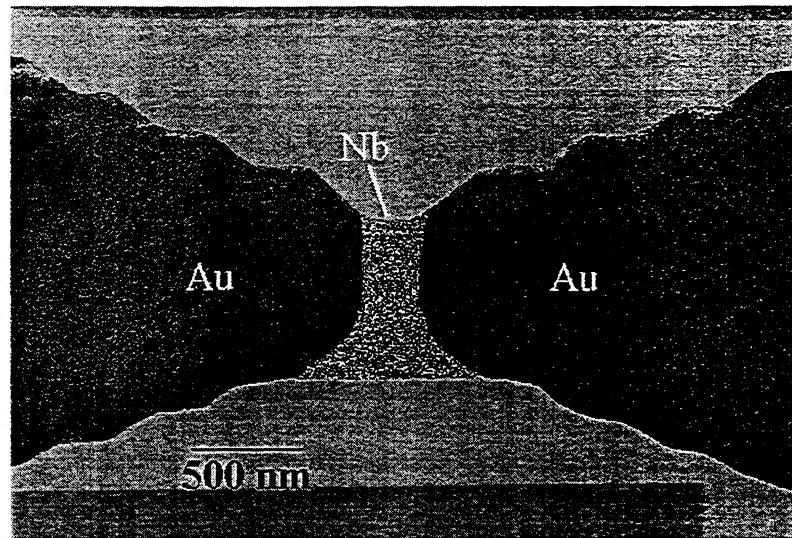
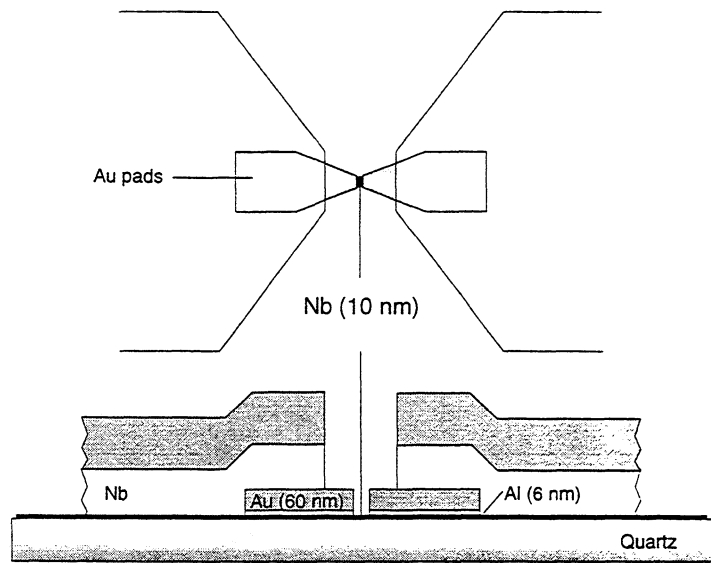


FIG. 1(a) schematic top and cross-sectional views of a hot-electron bolometer mixer; (b) SEM micrograph of the centre part of a completed HEB.

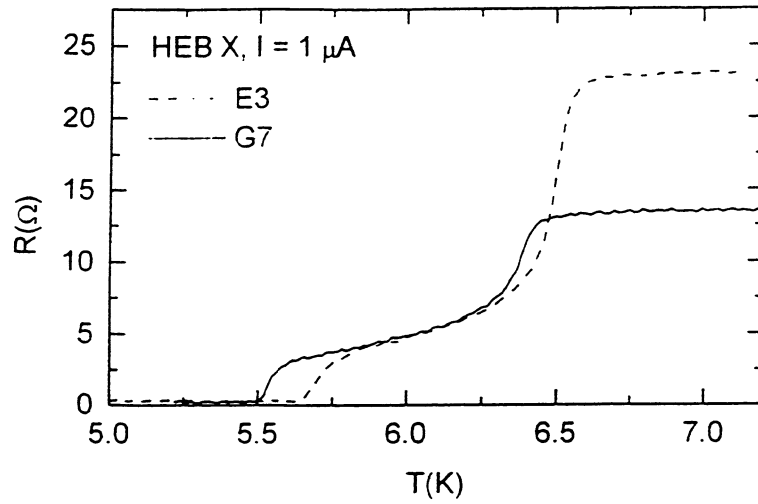


FIG. 2. Resistance as a function of temperature for two different HEBs. The temperature values, 5.5 K and 6.5 K, correspond to the T_c of the Nb under the Au pads and the T_c of the Nb bridge, respectively.

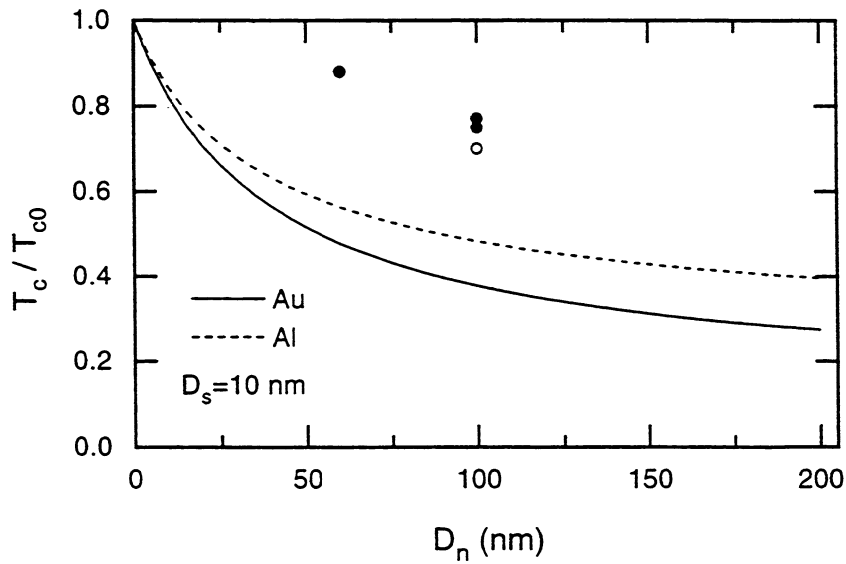


FIG. 3. Calculated normalized critical temperature T_c/T_{c0} of 10 nm thick Nb under a normal metal layer, which is either Au or Al layer, as a function of the thickness D_n . The curves are theoretical values and the data points are experimental values. The data point indicated by “ \circ ” is taken from ref. 11. T_{c0} is the original critical temperature of 10 nm thick Nb, that is 6.5 K in our case.

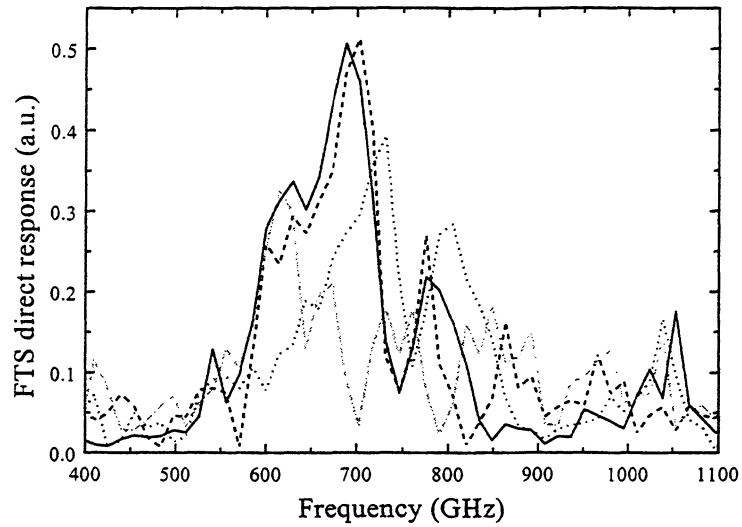


FIG. 4. FTS Spectra of a HEB mixer in a 750 GHz waveguide mixer block. Different curves correspond to measurements with different positions of the backshort tuner. The continuous curve corresponds to the case that the backshort is close to the HEB.

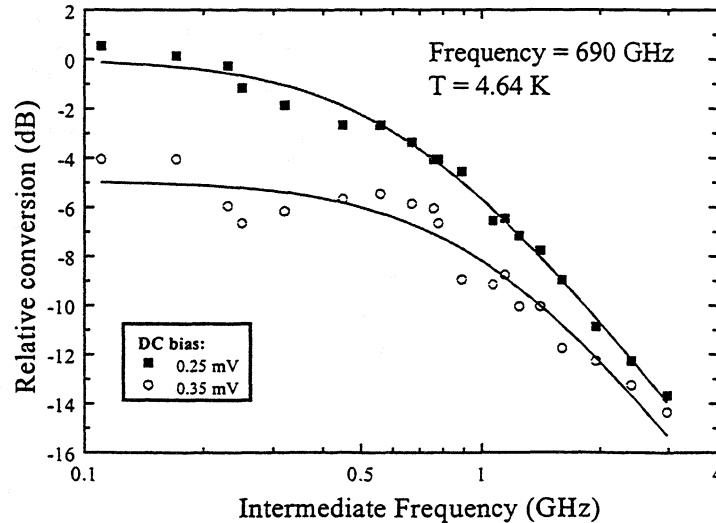


FIG. 5 Relative conversion efficiency of a HEB mixer is measured as a function of intermediate frequency at two bias voltages. The data points are the measurements and the curves are the fits (see the text).

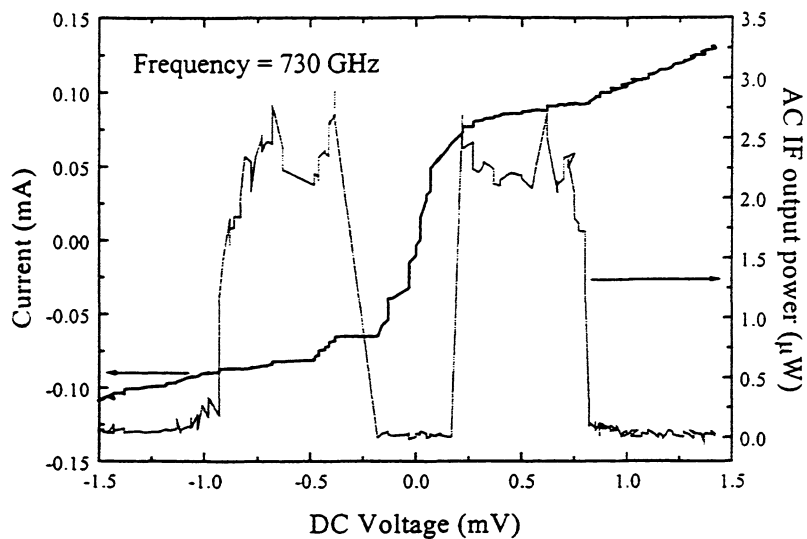


FIG. 6 AC IF output power of a HEB mixer, that responds to hot/cold load, as a function of DC bias voltage and the pumped I - V curve. Measurements are done at a LO frequency of 730 GHz and at a bath temperature of 4.6 K.